Greater oxidative susceptibility of the surface monolayer in small dense LDL may contribute to differences in copper-induced oxidation among LDL density subfractions[1]

Diane L. Tribble,[2,*] Ronald M. Krauss,[*] Maarten G. Lansberg,[*] Patrick M. Thiel,[*] and Jeroen J. M. van den Berg[†]

Department of Molecular and Nuclear Medicine, Life Science Division,[*] Lawrence Berkeley Laboratory, University of California, Berkeley, CA 94720, and Children's Hospital Oakland Research Institute,[†] Oakland, CA 94609

Abstract We monitored peroxidative stress in the surface monolayer as compared with the outer core of large, buoyant (d 1.025–1.032 g/ml) and small, dense (d 1.040–1.054 g/ml) low density lipoprotein (LDL) subfractions using the oxidation-labile fluorescent probes parinaric acid (PnA) and parinaric acid methyl ester (PnME), which partition preferentially into these respective regions of LDL. Oxidation was initiated either with $CuSO_4$ (5 μM) or the iron (Fe^{3+})-containing lipophilic complex hemin (1.0 μM) plus cumene hydroperoxide to facilitate heme degradation. In the presence of Cu^{2+}, PnA was depleted significantly more rapidly than PnME in dense ($P = 0.039$) but not in buoyant LDL, suggesting that surface vulnerability is enhanced in dense LDL particles. With hemin, PnA and PnME were similarly susceptible within both subfractions, although there was a trend toward slower loss of PnA in buoyant LDL ($P = 0.10$), consistent with the internal site of initiation and a greater surface resistance in buoyant particles. As indicated by conjugated diene lag times, dense LDL was more susceptible than buoyant LDL to oxidation by Cu^{2+} ($P = 0.03$) but not hemin ($P = 0.68$). These results suggest that the increased susceptibility of dense LDL to oxidation by external agents such as Cu^{2+} is at least partially mediated by an enhanced vulnerability of the surface compartment.—**Tribble, D. L., R. M. Krauss, M. G. Lansberg, P. M. Thiel, and J. J. M. van den Berg.** Greater oxidative susceptibility of the surface monolayer in small dense LDL may contribute to differences in copper-induced oxidation among LDL density subfractions. *J. Lipid Res.* 1995. **36:** 662–671.

Supplementary key words oxidation • fluorescent probes • large buoyant LDL • small dense LDL • hemin • parinaric acid

Oxidative modifications of LDL, produced by incubation with metabolically active cells and model oxidant systems (e.g., Cu^{2+}), alter the physicochemical properties and biological behavior of these particles, and thereby may facilitate their participation in atherogenic processes (1). Small, dense LDL are more susceptible to Cu^{2+}-induced oxidation than large, buoyant LDL (2–6), and this is suggested to contribute to the increased atherosclerosis risk associated with lipoprotein profiles relatively enriched in smaller (pattern B) as compared with larger (pattern A) LDL particles (7). Mechanisms underlying differences in oxidative susceptibility among LDL density subfractions remain poorly understood, but are likely to have broad implications with regard to determinants of LDL oxidative behavior and strategies for intervening in LDL oxidation in vivo, particularly in susceptible individuals.

The quasi-spherical LDL particle is organized into two major compartments, a hydrophobic core, comprised primarily of cholesteryl esters and triglycerides, surrounded by a surface monolayer of phospholipids with interdigitated free cholesterol (8–10). One copy of apolipoprotein B-100 is present per LDL particle, and is believed to wrap around the outer surface (11), with sites of hydrophobicity immersed in the lipid phase (12). Although little attention has been given to the influence of particle organization on LDL oxidative behavior, this feature is likely to play a major role in determining the course of oxidative changes, and, as we suggest, may be important to differences in oxidative susceptibility among LDL subfractions of differing density and particle size.

We previously reported that variations in Cu^{2+}-induced oxidation among LDL density subfractions correspond with variations in the content of free cholesterol (3), and the radical-scavenging antioxidants ubiquinol-10 and α-tocopherol (6), all of which are reduced in dense as com-

Abbreviations: LDL, low density lipoproteins; PnA, parinaric acid; PnME, parinaric acid methyl ester; CD, conjugated diene; cumOOH, cumene hydroperoxide; HAF, hexadecanoyl aminofluorescein.

[1]Preliminary results were presented at the annual meeting of the American Heart Association, Atlanta, GA, November 1993.

[2]To whom correspondence should be addressed.

pared with buoyant LDL. While the particle localization of ubiquinol-10 and α-tocopherol has not been established, like free cholesterol, these antioxidants are suggested to reside primarily within the LDL surface monolayer. Ubiquinol-10 shares metabolic precursors with and is structurally similar to free cholesterol, and thus is expected to show similar partitioning properties. A predominant surface localization is likewise proposed for α-tocopherol on the basis of its structural attributes and known ability to interact with aqueous hydrogen donors (e.g., ascorbic acid) (13, 14). Given this expected commonality in localization, and the association of these constituents with oxidative susceptibility, we hypothesized that the surface is the initial site of LDL injury by external oxidants such as Cu^{2+} and that this compartment is more susceptible in smaller, more dense LDL and may thus contribute to the greater overall oxidative susceptibility of these particles.

In the current studies, to test these hypotheses, we developed an approach for separately monitoring peroxidative stress in LDL surface and outer core compartments using parinaric acid (PnA), and a hydrophobic derivative, parinaric acid methyl ester (PnME), respectively. The course of oxidative probe depletion was compared in large, buoyant (d 1.025–1.032 g/ml) and small, dense (d 1.040–1.054 g/ml) LDL subfractions in response to either Cu^{2+} or the Fe^{3+}-containing porphyrin hemin. The lipophilic hemin molecule is expected to partition more deeply into LDL than Cu^{2+}, and thus to initiate oxidation from within the particle (15–18). As a result of differences in their sites of interaction with LDL, Cu^{2+} and hemin were predicted to differ in their effects on the oxidative behavior of surface and core parinaroyl probes and in their ability to promote an enhanced response in small, dense as compared with large, buoyant LDL.

METHODS

Chemicals

PnA (9,11,13,15-*cis-trans-trans-cis*-octadecatetraenoic acid) was obtained from Molecular Probes (Eugene, OR). PnME was synthesized from PnA using diazomethane as methylation agent, and was purified by semi-preparative reversed-phase HPLC on an ODS column (25 cm × 1 cm i.d., 5 μm particles) using methanol as solvent at 2.5 ml per min. Under these conditions, PnA eluted at 6.1 min, and a methylation product was collected at 12.4 min. The product was confirmed to be PnME using gas chromatography–mass spectrometry as described previously (19). PnME showed a characteristic electron impact mass spectrum with a molecular ion at *m/z* 290.

TROLOX (6-hydroxy-2,5,7,8-tetramethylchroman-2-carboxylic acid) was obtained from Aldrich Chemical Co. (Milwaukee, WI). EDTA, $CuSO_4$, hemin, cumene hydroperoxide, and deferoxamine mesylate were from Sigma Chemical Co. Hemin stock solutions were prepared fresh in 50 mM NaOH and diluted with phosphate-buffered saline (PBS). All reagents, buffer components, and HPLC solvents were of the highest grade commercially available.

Isolation and characterization of LDL subfractions

Blood was obtained from healthy normolipidemic adult volunteers not using vitamin supplements or taking hormones or drugs known to alter plasma lipids or lipoproteins. Samples were collected into Vacutainers containing 1 mg/ml EDTA. Cells were removed by centrifugation at 2000 *g* for 30 min under refrigeration (4°C), and 10 μM TROLOX was immediately added to plasma. LDL subfractions were isolated from separate plasma aliquots by sequential ultracentrifugation at d 1.026 g/ml and d 1.032 g/ml (for buoyant LDL) or d 1.040 g/ml and d 1.054 g/ml (for dense LDL) as previously described (6, 20). Subfractions were characterized according to particle diameter by nondenaturing 2–16% gradient gel electrophoresis (21), and lipid (phospholipid, triglyceride, cholesterol, and cholesteryl ester) and protein composition using standard methods (3, 6). Differences in physical and chemical characteristics between these buoyant and dense LDL preparations were as previously reported (6, 20).

Resonance energy transfer localization of parinaroyl probes

The fluorescent probes PnA and PnME were used to monitor site-specific peroxidative stress within the LDL particle. To assess their localization relative to the LDL surface, we examined resonance energy transfer to the surface acceptor molecule 5-(*N*-hexadecanoylamino)fluorescein (HAF) in experiments analogous to those previously described by Sklar et al. (22).

LDL oxidation studies

LDL subfractions were dialyzed for 48 h against four changes of 0.01 M PBS, pH 7.4, to remove NaBr, EDTA, and TROLOX. LDL oxidation was initiated by addition of either $CuSO_4$ (5 μM) or hemin (final concentrations ranging from 0.125 to 1.0 μM). For experiments involving Cu^{2+}, LDL protein concentrations were adjusted to 100 μg/ml. For experiments involving hemin, dense LDL was incubated at 100 μg protein/ml, and buoyant LDL was adjusted to obtain equal lipid concentrations. In some cases, cumene hydroperoxide (cumOOH) (1.0–10 μM) was used to promote hemin degradation (followed by monitoring the loss of absorbance at 412 nm) and to initiate lipid peroxidation, and deferoxamine (10 μM) was added to examine the effects of iron chelation. All incubations were carried out at 37°C.

To confirm that hemin was indeed taken up by LDL, we added 50 μM hemin to 1.5 mg LDL protein, reisolated

LDL by fast-protein liquid chromatography (FPLC) using two Sepharose 6 columns in series, and determined the extent to which hemin was recovered in the reisolated sample. Hemin concentrations were measured spectrophotometrically as a hemin-pyridine complex as previously described by Balla et al. (17).

Measures of LDL oxidation

Oxidative stress in LDL compartments was monitored by following the oxidative fluorescence loss of PnA and PnME. These probes were added to LDL by injections of small amounts of ethanolic solutions (ethanol never exceeded 0.5% v/v) to a final concentration of 0.85 μM in a total volume of 2 ml PBS (~5 probe molecules/LDL particle). As previously illustrated by Laranhinja, Almeida, and Madeira (23), these concentrations are ~5- to 10-fold lower than those at which fluorescence quenching is observed, thus ensuring that fluorescence intensity is linearly related to probe concentration and is not affected by small variations in LDL concentration or small differences in surface area between buoyant and dense LDL. As the unincorporated probes are minimally fluorescent in micelles due to self-quenching, incorporation into LDL can be monitored by following the appearance of a fluorescence signal. Probes were allowed to equilibrate, as indicated by signal stability, prior to oxidant addition. Initial fluorescence intensity was similar for buoyant and dense LDL indicating a similar degree of incorporation of the parinaroyl probes. Fluorescence measurements were performed using a Shimadzu RF-5000 Spectrofluorophotometer equipped with a thermostatted cuvette and a magnetic stirring device. Excitation and emission wavelengths were set at 324 nm (slit width 1.5 nm) and 413 nm (slit width 20 nm), respectively. Parinaroyl probe oxidation lag times were determined from the intersect of lines drawn through the initial slow phase and the linear portion of the rapid phase, and oxidation rates were determined from the slope of the rapid phase (6).

Conjugated diene (CD) formation was determined as an index of LDL lipid peroxidation by monitoring the increase in absorbance at 234 nm (24). Measurements were performed in a Shimadzu UV2101-PC scanning spectrophotometer equipped with a thermostatted 6-position automatic sample changer. Initial absorbance was set at zero and was recorded every 2 min for up to 8 h. Lag times were calculated from the time interval between initiation and the intercept of the tangent of the slope of the absorbance curve.

Statistical analyses

Statistical analyses were performed using the Statview II statistical program. Mean differences in lipid and protein composition, particle diameter, and CD lag times between LDL density subfractions, and parinaroyl probe lag times and intensity both within and between LDL subfractions were evaluated by paired-t analysis. Differences in resonance energy transfer efficiency from PnA and PnME to HAF were evaluated by comparing the percentage of parinaroyl fluorescence quenching across a range of HAF concentrations using repeated measures analysis-of-variance. All significance levels are based on two-tailed tests.

RESULTS

Particle localization of PnA and PnME in buoyant and dense LDL

PnA and PnME have been shown to differ in time-averaged localization within the LDL particle, with PnA at the surface and PnME in the outer core (22, 25). To confirm these expected sites of probe localization, and to identify any differences between buoyant and dense LDL, we examined resonance energy transfer from PnA and PnME to HAF. The chromophore of HAF resides at the lipoprotein surface at pH 7.4, and thus differences in energy transfer efficiency from PnA or PnME to HAF are believed to reflect differences in the depth of penetration of their respective chromophores.

The emission spectra of LDL-associated PnA and PnME were slightly different (**Fig. 1,** upper panel), particularly at wavelengths below the fluorescence maxima (413 nm), likely reflecting differences in probe environments. Notably, however, there were no differences within the range of wavelengths that overlapped with the absorption spectra of HAF (i.e., >420 nm, not shown), or the wavelength (413 nm) and probe intensity at fluorescence maxima (where oxidation studies are carried out). As shown in the lower panel of Fig. 1, at sufficiently high HAF concentrations, virtually all of the fluorescence of PnA was transferred to this acceptor (~90%), consistent with localization of PnA at the particle surface, i.e., in the surface monolayer. The extent of quenching of PnME fluorescence was ~40-50% lower in both buoyant and dense LDL at all HAF concentrations (P = 0.0001), indicating a significantly lower energy transfer efficiency and suggesting a greater penetration of PnME into the core of the particle. These results are similar to those of Sklar and colleagues (22) who calculated a depth of penetration of PnME consistent with a time-averaged localization within the outer core neighboring the surface monolayer. PnME fluorescence quenching was slightly, albeit significantly, greater in dense than buoyant LDL (~10% greater at 7.5 μM HAF; P = 0.001).

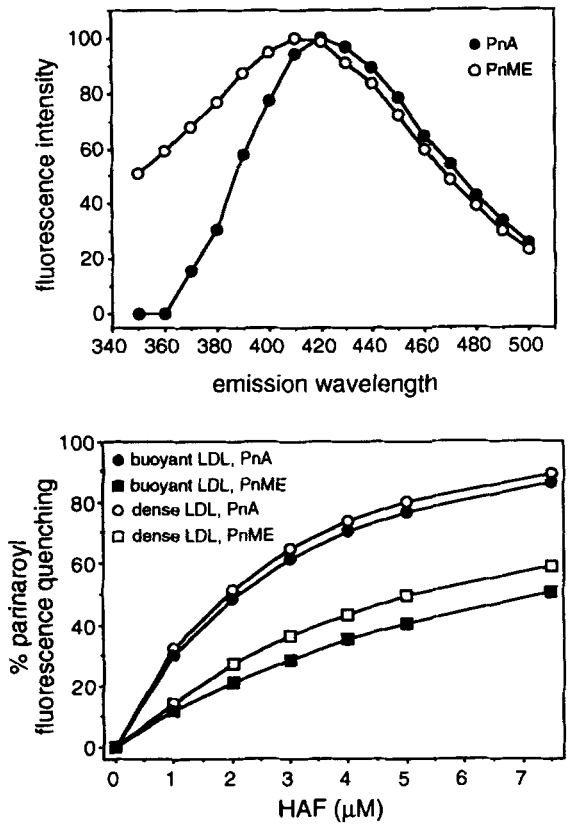

Fig. 1. Parinaroyl probe fluorescence properties in LDL. Upper panel: Emission spectra for PnA and PnME in LDL (ex: 324 nm). Results are shown for a representative dense LDL preparation; buoyant LDL exhibited a similar pattern. Lower panel: Probe localization was investigated by determining the effect of addition of increasing concentrations of a surface acceptor molecule, HAF, on parinaroyl fluorescence emission at 413 nm (ex: 324 nm). Resonance energy transfer from the parinaroyl probes to HAF was assessed from the percentage of parinaroyl probe fluorescence quenching, which was obtained by comparing fluorescence intensity in the presence and absence of HAF. Results are shown for a representative set of LDL subfractions.

Copper-induced depletion of PnA and PnME in buoyant and dense LDL

The course of Cu^{2+}-induced oxidation of PnA and PnME is shown in **Fig. 2** (upper panel) for a representative set of LDL subfractions. Fluorescence decay was characterized by an initial lag phase followed by an increased rate of loss until depletion. Loss of PnA preceded loss of PnME in dense but not buoyant LDL, suggesting a more susceptible surface monolayer pool in the former, and both probes were depleted more rapidly in dense than buoyant LDL. As we reported previously (6), parinaroyl probe loss occurs prior to the accelerated phase of CD formation (Fig. 2, lower panel), indicating that these probes are a more sensitive indicator of Cu^{2+}-induced peroxidative stress in the LDL particle.

The significance of differences in probe oxidative behavior in buoyant and dense LDL was determined by comparing PnA and PnME loss in eight sets of LDL subfractions (see **Table 1**). Based on lag times prior to accelerated probe depletion and rates of fluorescence loss in the accelerated phase (% change per min), PnA was more susceptible than PnME in dense LDL. In contrast, in buoyant LDL, PnA and PnME oxidation did not differ. Both probes were more labile in dense than buoyant LDL. A greater susceptibility of dense LDL also was indicated by shorter lag times prior to accelerated CD formation (see **Table 2**).

Characteristics of hemin-induced oxidation of buoyant and dense LDL

To evaluate the influence of site of initiation on parinaroyl probe behavior and differences in susceptibility among LDL density subfractions, we examined the effects of hemin, which in contrast to Cu^{2+} partitions into

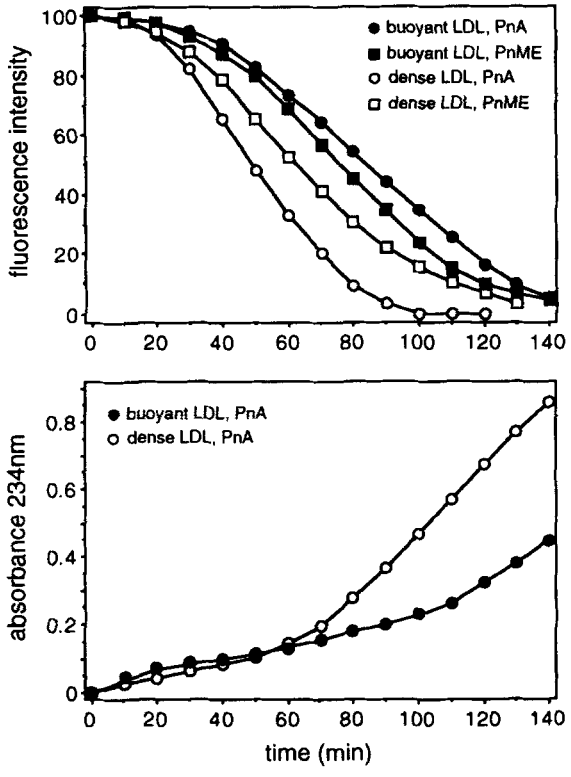

Fig. 2. Copper-induced oxidative fluorescence decay of PnA and PnME and conjugated diene formation in buoyant and dense LDL. Upper panel: PnA and PnME (1.0 μM final concentration) were added, in separate incubations, to buoyant and dense LDL and were allowed to equilibrate as indicated by fluorescence signal stability (ex: 324 nm; em: 413 nm). $CuSO_4$ (5 μM) was added to initiate oxidation, and parinaroyl fluorescence loss was followed for up to 3 h. Lower panel: CD formation was monitored by following the increase in absorbance at 234 nm. Results are shown for a representative set of LDL subfractions.

TABLE 1. *Lag times prior to and rates of fluorescence loss during the accelerated phase of parinaroyl probe oxidation in buoyant and dense LDL exposed to 5.0 μM $CuSO_4$*

LDL Subfraction	Lag Time			Rate of Loss in Accelerated Phase		
	PnA	PnME	PnA vs. PnME	PnA	PnME	PnA vs. PnME
	min			*%/min*		
Buoyant LDL	34.0 ± 4.8	36.2 ± 5.1	0.976	0.53 ± 0.14	0.44 ± 0.12	0.301
Dense LDL	18.5 ± 3.0	26.2 ± 4.7	0.039	0.93 ± 0.27	0.60 ± 0.14	0.162
Buoyant vs. dense LDL (*P* values)	0.004	0.048		0.028	0.050	

Values expressed are mean ± SE for eight sets of LDL subfractions. Significance levels (*P* values) for PnA vs. PnME and buoyant vs. dense LDL were derived using paired-*t* analysis.

and thus initiates oxidation from within the LDL particle. LDL internalization of hemin was supported by observations that virtually all (80–100%) added hemin was recovered in LDL after reisolation by FPLC. As a result of its internalization, the effective concentration of hemin was highly dependent on LDL concentration. Variations in oxidative response could be achieved either by varying the absolute concentration of hemin or of its LDL host (data not shown), suggesting that the latter determined the volume of distribution of hemin. As lipid mass is ~10–15% greater in buoyant than dense particles, in subsequent experiments, subfractions were adjusted to achieve similar lipid mass thus assuring equal volumes of distribution and effective concentrations of hemin. This adjustment does not hinder comparisons with experiments involving Cu^{2+} because subfraction-dependent differences in susceptibility to Cu^{2+}-induced oxidation are virtually identical when adjusted either according to protein or cholesterol content (D. L. Tribble, R. M. Krauss, and A. Chait, unpublished observations). Notably, evaluation of hemin-induced oxidation in three sets of LDL subfractions did not show any differences under isolipid versus isoprotein conditions, likely due to the fact that the adjustments in LDL concentration are relatively small in relation to interindividual variations in responsiveness.

Figure 3 shows the course of CD formation in a representative dense LDL subfraction exposed to 0.125, 0.250, and 1.0 μM hemin (<1 to 5 molecules per LDL particle). Hemin-induced LDL oxidation differed from Cu^{2+}-induced LDL oxidation in several notable ways. Lag times prior to CD formation did not differ as a function of initial hemin concentration, but the extent of changes (as indicated by the maximal absorbance at 234 nm) varied approximately 3-fold over this range, with no differences observed between buoyant and dense LDL. In contrast, variations in Cu^{2+} concentrations from 1.66 to 10 μM were accompanied by variations in lag times over a 2-fold range, but not in the extent of changes ultimately achieved (data not shown). Maximal values in hemin-exposed LDL remained stable for up to 8 h, and thus did not achieve the levels obtained with Cu^{2+} (~1.6 absorbance units), although subsequent addition of either Cu^{2+} or hemin produced further rapid increases, suggesting that the plateau was not due to depletion of oxidizable lipid substrates. Hemin-derived iron may have been converted into a form unable to promote further oxidation. Higher initial concentrations of hemin (>1.0 μM) did not result in greater maximal absorbance values, possibly because decomposition of lipid hydroperoxides also was enhanced under these conditions.

Hemin-induced LDL oxidation requires initial degradation of the heme ring, presumably with release of catalytically active iron (17, 18). We observed considerable variation in the course of hemin degradation between

TABLE 2. Lag time estimates and maximal values obtained for A_{234nm}-absorbing species (conjugated dienes) in buoyant and dense LDL exposed to $CuSO_4$ (5.0 μM), hemin (1.0 μM), or hemin/cumOOH (1.0 μM/1.0 μM)

LDL Subfraction	$CuSO_4$ (n = 10)		Hemin (n = 5)		Hemin/cumOOH (n = 5)	
	Lag Time (min)	Max. Abs. 234nm	Lag Time (min)	Max. Abs. 234nm	Lag Time (min)	Max. Abs. 234nn
Buoyant LDL	121.0 ± 19.4	1.49 ± 0.27	150.2 ± 52.1	0.71 ± 0.15	51.0 ± 28.2	0.45 ± 0.07
Dense LDL	87.7 ± 12.0	1.38 ± 0.16	83.7 ± 21.5	0.73 ± 0.12	48.8 ± 22.9	0.66 ± 0.19
Buoyant vs. dense LDL (*P* values)	0.015	0.295	0.093	0.943	0.845	0.065

Values expressed are mean ± SE. Significance levels (*P* values) for differences between buoyant and dense LDL were derived using paired-*t* analysis.

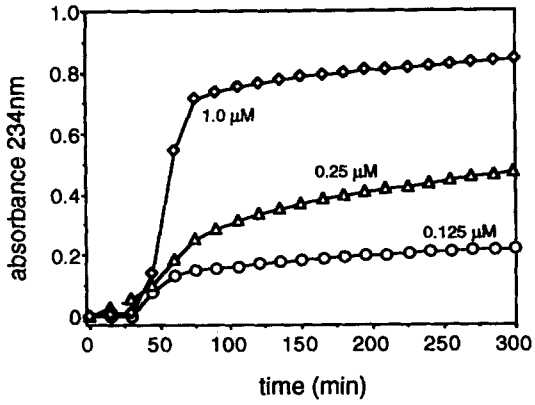

Fig. 3. Conjugated diene formation in LDL in response to three concentrations of hemin. Hemin was added to LDL to final concentrations of 0.125, 0.250, and 1.0 μM. CD formation was monitored by following the increase in absorbance at 234 nm. Results are shown for a representative dense LDL preparation; the pattern and extent of response to hemin were similar in buoyant LDL.

LDL preparations (i.e., between subjects), as indicated by the decrease in absorbance at 412 nm (values ranged from 30 to 300 min). To minimize interindividual variation and to ensure that the proximate oxidant was generated in buoyant and dense particles at identical rates, we added small amounts of hydroperoxide, as previously described (17, 18). In keeping with our aim of promoting oxidation internally, we used the lipophilic agent cumene hydroperoxide (cumOOH), which elicited a concentration-dependent increase in the rate of hemin degradation from 1.0 to 10 μM (**Fig. 4**). In subsequent experiments, we used 1.0 μM hemin together with 1.0 μM cumOOH to initiate LDL oxidation. Under these conditions, the course of hemin degradation was similar in buoyant and dense LDL (**Fig. 5**, upper panel). CD lag times also were reduced by

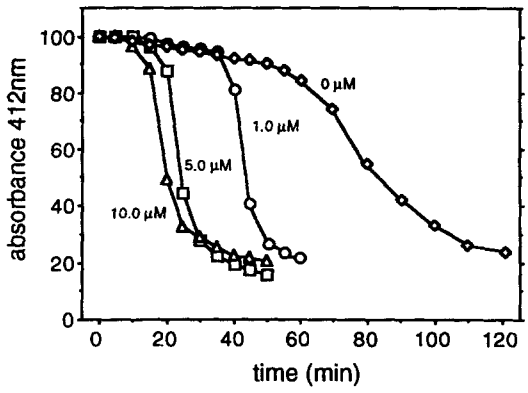

Fig. 4. Effect of cumene hydroperoxide concentration on hemin degradation in LDL. Hemin was added to LDL to a final concentration of 1.0 μM. CumOOH was either excluded or added to final concentrations of 1.0, 5.0, or 10.0 μM. Hemin degradation was monitored by following the loss in absorbance at 412 nm. For clarity, results are shown for dense LDL only; a similar pattern was observed for buoyant LDL.

cumOOH, in close correspondence with acceleration of hemin degradation, and differences between subfractions were eliminated (Fig. 5, lower panel; Table 2).

It is unlikely that addition of cumOOH directly altered the oxidative response of hemin-containing LDL. This agent had no effect in the absence of hemin and addition of the iron chelator deferoxamine (10 μM) completely inhibited CD formation in both hemin- and hemin/cumOOH-exposed LDL, even though hemin degradation still proceeded under these conditions (data not shown). The inhibitory effects of deferoxamine appeared to be due to iron chelation since ferrioxamine (iron-saturated deferoxamine) caused only a slight (20–30%) delay in hemin-induced LDL oxidation. These results indicate that released iron is essential for initiating oxidation in hemin/cumOOH-exposed LDL and that no significant oxidative damage results directly from the interaction of cumOOH with hemin.

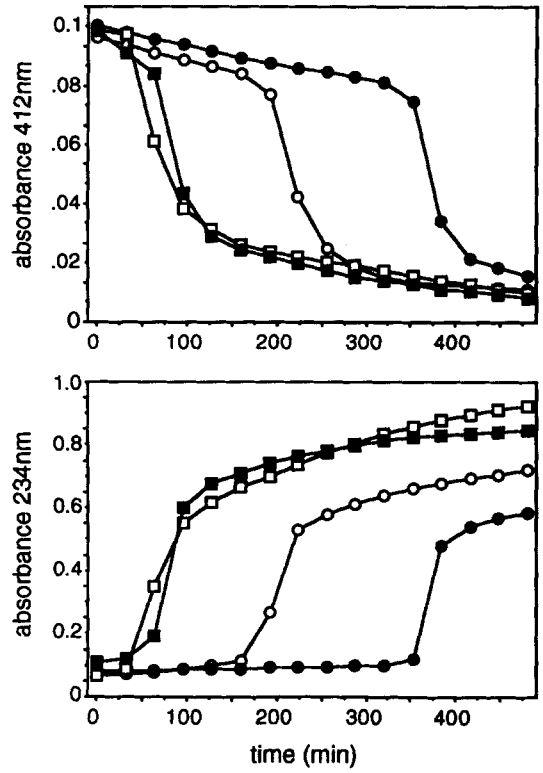

Fig. 5. Hemin degradation and conjugated diene formation in buoyant and dense LDL exposed to hemin/cumene hydroperoxide. Hemin was added to buoyant (closed symbols) and dense (open symbols) LDL subfractions to a final concentration of 1.0 μM. CumOOH was either excluded (circles) or added to a final concentration of 1.0 μM (squares). Hemin degradation was monitored by following the loss in absorbance at 412 nm (upper panel). CD formation was monitored by following the increase in absorbance at 234 nm (lower panel). Results are shown for a representative set of LDL subfractions, although subfraction differences in hemin degradation and CD formation in the absence of cumOOH in this particular sample were larger than average (see Table 2).

In contrast to results with hemin, neither cumOOH (1 μM) nor hydrogen peroxide (H_2O_2) (25 μM) accelerated oxidation in Cu^{2+}-exposed LDL (data not shown). Rather, in some experiments, addition of hydroperoxide actually appeared to slow the course of Cu^{2+}-induced CD formation, particularly in buoyant LDL, thus increasing rather than decreasing differences between LDL density subfractions.

Hemin-induced depletion of PnA and PnME in buoyant and dense LDL

On the basis of differences in site of interaction with the LDL particle, we postulated that hemin would differ from Cu^{2+} in its effects on the sequential oxidative loss of surface- and core-localized parinaroyl probes. The course of PnA and PnME depletion by hemin/cumOOH is shown in **Fig. 6** (upper panel) for a representative set of LDL subfractions. PnME appeared to be depleted more readily than PnA in both buoyant and dense LDL subfractions, consistent with an internal site of initiation. As with CD formation (Fig. 6, lower panel), oxidation of PnA and PnME did not go to completion in hemin-exposed LDL. In contrast to results obtained with Cu^{2+}, parinaroyl probe depletion occurred in tandem with CD formation.

The significance of differences in probe behavior induced by hemin/cumOOH was evaluated for five sets of LDL subfractions. Due to the hyperbolic nature of probe oxidation in hemin-exposed LDL, it was not possible to derive lag times or oxidation rates in some preparations. Therefore, for comparison, we used % residual parinaroyl fluorescence at 1 h. Based on this index, depletion rates for PnA as compared with PnME were not significantly different within either buoyant or dense LDL (52.6 $\pm$ 5.3 vs. 41.5 $\pm$ 7.5 in buoyant LDL; 39.8 $\pm$ 7.6 vs. 40.0 $\pm$ 8.6 in dense LDL). However, there was a trend toward greater resistance of PnA than PnME within buoyant LDL (P = 0.104), and PnA was more resistant in buoyant than dense LDL (P = 0.042).

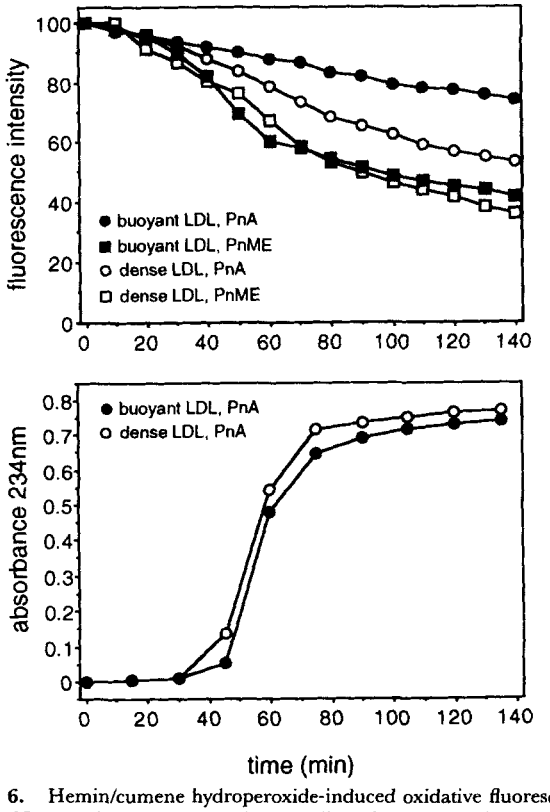

Fig. 6. Hemin/cumene hydroperoxide-induced oxidative fluorescence loss of PnA and PnME and conjugated diene formation in buoyant and dense LDL. Upper panel: PnA and PnME (1.0 μM final concentration) were added, in separate incubations, to buoyant and dense LDL and were allowed to equilibrate as indicated by fluorescence signal stability (ex: 324 nm; em: 413 nm). Oxidation was initiated by addition of hemin (1.0 μM) followed by cumOOH (1.0 μM), and parinaroyl fluorescence loss was followed for up to 3 h. Lower panel: CD formation was monitored by following the increase in absorbance at 234 nm. Results are shown for a representative set of LDL subfractions.

DISCUSSION

To evaluate the role of the surface monolayer as a determinant of susceptibility of LDL to oxidation induced by external agents (e.g., Cu^{2+}), especially as it pertains to differences in susceptibility among LDL density subfractions, we developed an approach using the oxidation-labile fluorescent probes PnA and PnME to separately monitor peroxidative stress in LDL surface and core compartments. Site-specific oxidative changes in LDL have been examined by comparing rates of formation of surface and core lipid oxidation products including phospholipid and cholesteryl ester hydroperoxides (26-28), and cholesterol and cholesteryl ester oxidation products (29). However, despite the obvious advantages of measuring endogenous lipids, these measurements reflect steady-state levels and may be affected by oxidative decomposition. Although not endogenous components, parinaroyl probes provide a simple and direct means of monitoring peroxidative stress within LDL (6, 23, 30-33). Moreover, because this assay does not involve product measurement, it is not affected by decomposition reactions.

Particle localization of the parinaroyl probes was assigned on the basis of resonance energy transfer to a surface acceptor molecule. The efficiency of energy transfer between two fluorescent probes that display overlapping emission (donor) and absorption (acceptor) spectra is highly dependent on the physical distance between the probes. We used HAF as the surface acceptor, and compared its interaction with PnA and PnME as an index of the relative distance of these two probes from the particle surface. Results showed that PnA is more effective than PnME in communicating with HAF, consistent with a time-averaged localization closer to the particle surface.

These results are similar to those of Sklar et al. (22) in which they calculated that PnA was located in the surface monolayer and PnME was located approximately 20 Å from the HAF fluorophore in a zone they referred to as the "outer core." PnME fluorescence quenching was slightly greater in dense than buoyant LDL possibly reflecting increased effective probe concentrations due to the decreased surface area and volumes of the monolayer and core. In addition, a greater proportion of PnME may have partitioned into the surface monolayer of smaller LDL particles. It should be noted that even though they have a preferred region of localization, both probes are expected to be capable of movement throughout the particle. Indeed, we have observed that PnME can exchange between lipoproteins (D. L. Tribble, E. L. Gong, J. J. M. van den Berg, F. van Venrooij, and A. V. Nichols, unpublished observations), suggesting that PnME is present in the surface monolayer from which it can desorb for exchange. Substantial presence of probes outside of their preferred site of localization would tend to make the observed differences in surface and core oxidative behavior an underestimation of the actual differences.

Oxidation was initiated either with Cu^{2+} or hemin, a lipophilic Fe^{3+}-containing complex. While Cu^{2+} and Fe^{3+} are chemically distinct, it was our premise that the primary difference between these two oxidants is in their site of interaction with the LDL particle. Our use of these oxidants, as opposed to the hydrophilic and lipophilic azo radical initiators 2,2'-azobis(2-amidinopropane) dihydrochloride (AAPH) and 2,2-azobis(2,4-dimethylvaleronitrile) (AMVN), was based on two major factors. First and foremost, while azo initiators are advantageous in that radical production can be carefully controlled, concentrations used to achieve a sufficient rate of LDL oxidation have been quite high (i.e., 1.0–2.0 mM) (26–28). In the case of the lipophilic initiator (AMVN), this could amount to the incorporation of as many as 10^3 to 10^4 molecules on average into each LDL particle, depending on LDL concentration. This is particularly striking given that the total number of lipid molecules per LDL particle is estimated to be within this range (24). Such oxidant loading is likely to profoundly affect molecular interactions within the LDL particle, and thereby to artefactually influence the properties that we are attempting to understand. Hemin, in contrast, was added to final concentrations ranging from < 1 to 5 molecules per LDL particle. It is unlikely that substantial particle disruption occurred under these circumstances. Secondly, much of our understanding of LDL oxidation to date has been obtained using metals, including studies indicating differences in the oxidative behavior of LDL density subfractions, thus allowing comparisons of the present results with previous findings (2–6).

Peroxidative stress induced by Cu^{2+} is "sensed" by PnA prior to PnME in dense LDL particles, suggesting that injury starts at the surface and progresses inward. In contrast, in buoyant LDL, differences in Cu^{2+}-induced oxidation of surface and core probes were not perceptible, and both were more resistant than in dense LDL. When oxidation was initiated by hemin, with simultaneous addition of cumOOH to facilitate degradation of the heme ring, core probe oxidation appeared to precede surface probe oxidation, particularly within the buoyant LDL particle, although such differences in probe behavior were not significant. The core probe was equally susceptible to hemin-induced oxidation in buoyant and dense LDL, but differences in surface probe behavior between subfractions still were apparent under these conditions.

The enhanced response of the surface probe as compared with the core probe in Cu^{2+}-exposed LDL appears to contradict previous reports indicating that cholesteryl ester hydroperoxides accumulate at rates similar to or greater than phospholipid hydroperoxides, even in the presence of external oxidants (26–28). It appears possible that this discrepancy is explained in large part by our use of LDL subfractions since the enhanced response in our studies was specific to small, dense LDL particles. LDL from most individuals is comprised primarily of the subspecies LDL-I and LDL-II (34). In unfractionated LDL preparations, these subspecies may determine the overall response (3) and may thus mask the behavior of LDL-III, which is the predominant particle in our dense LDL fraction (6, 20). Another factor possibly contributing to differences between the current and previous results lies in the fact that the parinaroyl probe assay is not affected by decomposition reactions. We suggest that the relative extent of cholesteryl ester versus phospholipid hydroperoxide accumulation may be influenced by the relative susceptibility of these products to oxidative decomposition. Surface-localized phospholipid hydroperoxides are predicted to be more vulnerable to decomposition than cholesteryl ester hydroperoxides.

LDL was more susceptible to oxidation by hemin/cumOOH than Cu^{2+}, as indicated by similar CD lag times at concentrations that were 5- to 40-fold lower (0.125 to 1.0 μM vs. 5 μM), although the extent of changes was reduced in the former. We believe that the greater susceptibility of LDL to hemin is due primarily to the internal site of initiation. Internalized agents such as hemin may impose a greater oxidant stress due to the smaller volume of distribution and thus higher effective concentration and/or may be more effective as a result of being in closer proximity to oxidizable substrates. The response to these agents may be further enhanced by a reduced intrinsic resistance of the lipoprotein to oxidative stress generated from within the particle. The antioxidants ubiquinol-10

and α-tocopherol, for example, could be less effective in protecting core than surface lipids due to a predominant localization within the surface monolayer. A reduced role for surface monolayer constituents in determining the oxidative response to hemin/cumOOH could account for the lack of differences in oxidative susceptibility between buoyant and dense LDL under these conditions.

Differences in the chemical properties of Cu^{2+} and hemin also likely contributed to the observed differences in their effectiveness in promoting LDL oxidation, particularly with regard to the lower total response in hemin-exposed LDL. Lynch and Frei (35) recently reported that Fe^{3+}-citrate does not induce LDL oxidation in the absence of superoxide anion (O_2^-), which they proposed was required for the reduction of Fe^{3+} to Fe^{2+}. Although hemin-induced LDL oxidation is not dependent on an external reductant (present results, refs. 17, 18), accumulation of iron in a nonoxidizing form may have contributed to the lower extent of oxidation.

In conclusion, we observed that the oxidative response of PnA, used as an index of surface susceptibility, differed in buoyant and dense LDL in the presence of both Cu^{2+} and hemin. A greater susceptibility of surface monolayer constituents in dense LDL may contribute to the enhanced susceptibility of these particles to oxidation by external agents. The physiological relevance and therapeutic implications of these findings depend on the oxidizing conditions encountered in vivo. If external oxidants are the predominant mediators of LDL oxidation in vivo, then surface properties may be particularly important determinants of LDL oxidation, and the surface may thus represent the most appropriate site for intervening in the oxidation process, particularly in individuals with lipoprotein profiles enriched in smaller, more dense LDL particles.

This research was supported by NIH grants HL18574, HL27059 and DK32094 and a grant from the National Dairy Promotion and Research Board administered in cooperation with the National Dairy Council (to R.M.K.), and was conducted at Lawrence Berkeley Laboratory through the U.S. Department of Energy under contract No. DE-AC03-76SF00098. D.L.T. and J.v.d.B. were supported by funds from the Tobacco-Related Disease Research Program of the University of California (Grants KT-106 and 4KT-0265). The authors wish to thank Dr. N. E. Cook, F. van Venrooij, and K. Hamoen for technical assistance, and Dr. F. A. Kuypers for helpful discussions.

Manuscript received 16 May 1994 and in revised form 18 October 1994.

REFERENCES

1. Steinberg, D., S. Parthasarathy, T. E. Carew, J. C. Khoo, and J. L. Witztum. 1988. Beyond cholesterol. Modifications of low-density lipoprotein cholesterol that increase its atherogenicity. *N. Engl. J. Med.* **320:** 915–924.
2. De Graaf, J., H. L. M. Hak-Lemmers, M. P. C. Hectors, P. N. M. Demarker, J. C. M. Hendriks, and A. F. H. Stalenhoef. 1991. Enhanced susceptibility to in vitro oxidation of the dense low density lipoprotein subfraction in healthy subjects. *Arterioscler. Thromb.* **11:** 298–306.
3. Tribble, D. L., L. G. Holl, P. D. Wood, and R. M. Krauss. 1992. Variations in oxidative susceptibility among six low density lipoprotein subfractions of varying size and density. *Atherosclerosis.* **93:** 189–199.
4. Chait, A., R. L. Brazg, D. L. Tribble, and R. M. Krauss. 1993. Susceptibility of small, dense low density lipoproteins to oxidative modification in subjects with the atherogenic lipoprotein phenotype, pattern B. *Am. J. Med.* **94:** 350–356.
5. Dejager, S., E. Bruckert, and M. J. Chapman. 1993. Dense low density lipoprotein subspecies with diminished oxidative resistance predominate in combined hyperlipidemia. *J. Lipid Res.* **34:** 295–308.
6. Tribble, D. L., J. J. M. van den Berg, P. Motchnik, B. N. Ames, D. Lewis, A. Chait, and R. M. Krauss. 1994. Oxidative susceptibility of low density lipoprotein subfractions is related to their ubiquinol-10 and α-tocopherol content. *Proc. Natl. Acad. Sci. USA.* **94:** 1183–1187.
7. Austin, M. A., J. L. Breslow, C. H. Hennekens, J. E. Buring, W. C. Willet, and R. M. Krauss. 1988. Low-density lipoprotein subclass patterns and risk of myocardial infarction. *J. Am. Med. Assoc.* **260:** 1917–1922.
8. Atkinson, D., R. J. Deckelbaum, D. M. Small, and G. G. Shipley. 1977. Structure of human plasma low-density lipoproteins: molecular organization of the central core. *Proc. Natl. Acad. Sci. USA.* **74:** 1042–1046.
9. Deckelbaum, R. J., G. G. Shipley, and D. M. Small. 1977. Structure and interactions of lipids in human plasma low density lipoproteins. *J. Biol. Chem.* **252:** 744–754.
10. Ginsburg, G. S., M. T. Walsh, D. M. Small, and D. Atkinson. 1984. Reassembled plasma low density lipoproteins. Phospholipid-cholesterol ester-apoprotein B complex. *J. Biol. Chem.* **259:** 6667–6673.
11. Chatterton, J. E., M. L. Phillips, L. K. Curtiss, R. W. Milne, Y. L. Marcel, and V. N. Schumaker. 1991. Mapping apolipoprotein B on the low density lipoprotein surface by immunoelectron microscopy. *J. Biol. Chem.* **266:** 5955–5962.
12. Yang, C-Y., Z-W. Gu, S-A. Weng, T. W. Kim, S-H. Chen, H. J. Pownall, P. M. Sharp. S-W. Liu, W-H. Li, A.M. Gotto, Jr., and L. Chan. 1989. Structure of apolipoprotein B-100 of human low density lipoprotein. *Arteriosclerosis.* **9:** 96–108.
13. Jialal, I., and S. M. Grundy. 1991. Preservation of the endogenous antioxidants in low density lipoprotein by ascorbate but not probucol during oxidative modification. *J. Clin. Invest.* **87:** 597–601.
14. Sato, K., E. Niki, and H. Shimasaki. 1991. Free radical-mediated chain oxidation of low density lipoprotein and its synergistic inhibition by vitamin E or vitamin C. *Arch. Biochem. Biophys.* **279:** 402–405.
15. Light, W. R., and J. S. Olson. 1990. Transmembrane movement of heme. *J. Biol. Chem.* **265:** 15623–15631.
16. Light, W. R., and J. S. Olson. 1990. The effects of lipid composition on the rate and extent of heme binding to membranes. *J. Biol. Chem.* **265:** 15632–15637.
17. Balla, G., H. S. Jacob, J. W. Eaton, J. D. Belcher, and G. M. Vercellotti. 1991. Hemin: a possible physiological mediator of low density lipoprotein oxidation and endothelial injury. *Arterioscler. Thromb.* **11:** 1700–1711.
18. Belcher, J. D., J. Balla, G. Balla, D. R. Jacobs, M. Gross, H. S. Jacob, and G. M. Vercellotti. 1993. Vitamin E, LDL,

and endothelium. Brief oral vitamin supplementation prevents oxidized LDL-mediated vascular injury. *Arterioscler. Thromb.* **13:** 1779–1789.
19. van den Berg, J. J. M., J. A. F. Op den Kamp, B. H. Lubin, and F. A. Kuypers. 1993. Conformational changes in oxidized phospholipids and their preferential hydrolysis by phospholipase A_2: a monolayer study. *Biochemistry.* **32:** 4962–4967.
20. Reaven, P. D., B. J. Grasse, and D. L. Tribble. 1994. Effects of linoleate-rich and oleate-rich diets in combination with α-tocopherol on the susceptibility of low-density lipoproteins (LDL) and LDL subfractions to oxidative modification in humans. *Arterioscler. Thromb.* **14:** 557–566.
21. Krauss, R. M., and D. J. Burke. 1982. Identification of multiple subclasses of plasma low density lipoprotein in normal humans. *J. Lipid Res.* **23:** 97–104.
22. Sklar, L. A., M. C. Doody, A. M. Gotto, and H. J. Pownall. 1980. Serum lipoprotein structure: resonance energy transfer localization of fluorescent probes. *Biochemistry.* **19:** 1294–1301.
23. Laranjinha, J. A. N., L. M. Almeida, and V. M. C. Madeira. 1992. Lipid peroxidation and its inhibition in low density lipoproteins: quenching of *cis*-parinaric acid fluorescence. *Arch. Biochem. Biophys.* **297:** 147–154.
24. Esterbauer, H., J. Gebicki, H. Puhl, and G. Jurgens. 1992. The role of lipid peroxidation and antioxidants in oxidative modification of LDL. *Free Radical Biol. Med.* **13:** 341–390.
25. Ben-Yasher, V., and Y. Barenholz. 1991. Characterization of the core and surface of human plasma lipoproteins: a study based on the use of five fluorophores. *Chem. Phys. Lipids.* **60:** 1–14.
26. Noguchi, N., N. Gotoh, and E. Niki. 1993. Dynamics of oxidation of low density lipoprotein induced by free radicals. *Biochim. Biophys. Acta.* **1168:** 348–357.
27. Bowry, V. W., K. U. Ingold, and R. Stocker. 1992. Vitamin E in human low-density lipoprotein. When and how this antioxidant becomes a pro-oxidant. *Biochem. J.* **288:** 341–344.
28. Frei, B., and J. M. Gaziano. 1993. Content of antioxidants, preformed lipid hydroperoxides, and cholesterol as predictors of the susceptibility of human LDL to metal ion-dependent and -independent oxidation. *J. Lipid Res.* **34:** 2135–2145.
29. Kritharides, L., W. Jessup, J. Gifford, and R. T. Dean. 1993. A method for defining the stages of low-density lipoprotein oxidation by the separation of cholesterol and cholesteryl ester-oxidation products using HPLC. *Anal. Biochem.* **213:** 79–89.
30. Kuypers, F. A., J. J. M. van den Berg, C. Schalkwijk, B. Roelofsen, and J. A. F. Op den Kamp. 1987. *Cis*-parinaric acid as a fluorescent membrane probe to determine lipid peroxidation. *Biochim. Biophys. Acta.* **921:** 266–274.
31. van den Berg, J. J. M., F. A. Kuypers, J. H. Qju, B. Lubin, B. Roelofsen, and J. A. F. Op den Kamp. 1988. The use of *cis*-parinaric acid to determine lipid peroxidation in human erythrocyte membranes. Comparison of normal and sickle erythrocyte membranes. *Biochim. Biophys. Acta.* **944:** 29–39.
32. van den Berg, J. J. M., J. A. F. Op den Kamp, B. H. Lubin, B. Roelofsen, and F. A. Kuypers. 1992. Kinetics and site specificity of hydroperoxide-induced oxidative damage in red blood cells. *Free Radical Biol. Med.* **12:** 487–498.
33. van den Berg, J. J. M., F. A. Kuypers, B. Roelofsen, and J. A. F. Op den Kamp. 1990. The cooperative action of vitamins E and C in the protection against peroxidation of parinaric acid in human erythrocyte membranes. *Chem. Phys. Lipids.* **53:** 309–320.
34. Musliner, T. A., and R. M. Krauss. 1988. Lipoprotein subspecies and risk of coronary disease. *Clin. Chem.* **33:** B78–B83.
35. Lynch, S. M., and B. Frei. 1993. Mechanisms of copper- and iron-dependent oxidative modification of human low density lipoprotein. *J. Lipid Res.* **34:** 1745–1753.